Synthesis and biological evaluation of radioiodinated 2,5-diphenyl-1,3,4-oxadiazoles for detecting β-amyloid plaques in the brain

Hiroyuki Watanabe[1], Masahiro Ono[1,2*], Ryoichi Ikeoka[1], Mamoru Haratake[1], Hideo Saji[2] and Morio Nakayama[1*]

[1]*Graduate School of Biomedical Sciences, Nagasaki University, 1-14 Bunkyo-machi, Nagasaki 852-8521,* [2]*Graduate School of Pharmaceutical Sciences, Kyoto University, 46-29 Yoshida Shimoadachi-cho, Sakyo-ku, Kyoto 606-8501, JAPAN.*

*To whom correspondence should be addressed: Phone +81-75-753-4608, Fax: +81-75-753-4568, e-mail: ono@pharm.kyoto-u.ac.jp for M. Ono. Phone: +81-95-819-2441, Fax: +81-95-819-2441, e-mail: morio@nagasaki-u.ac.jp for M. Nakayama.

Abstract

This paper describes the synthesis and biological evaluation of a new series of 2,5-diphenyl-1,3,4-oxadiazole (1,3,4-DPOD) derivatives for detecting β-amyloid plaques in Alzheimer's brains. The affinity for β-amyloid plaques was assessed by an *in vitro* binding assay using pre-formed synthetic Aβ42 aggregates. The new series of 1,3,4-DPOD derivatives showed affinity for Aβ42 aggregates with K_i values ranging from 20 to 349 nM. The 1,3,4-DPOD derivatives clearly stained β-amyloid plaques in an animal model of Alzheimer's disease, reflecting the affinity for Aβ42 aggregates *in vitro*. Compared to 3,5-diphenyl-1,2,4-oxadiazole (1,2,4-DPOD) derivatives, they displayed good penetration of and fast washout from the brain in biodistribution experiments using normal mice. The novel radioiodinated 1,3,4-DPOD derivatives may be useful probes for detecting β-amyloid plaques in the Alzheimer's brain.

1. Introduction

Alzheimer's disease (AD) is a progressive neurodegenerative disorder pathologically characterized by the deposition of β-amyloid (Aβ) peptides as senile plaques in the brain.[1,2] Since the deposition of Aβ plaques is an early event in the development of AD, a validated biomarker of Aβ deposition in the brain would likely prove useful for identifying and following individuals at risk for AD and assist in the evaluation of new anti-amyloid therapies currently under development. Therefore, the quantitative evaluation of Aβ plaques in the brain with non-invasive techniques such as positron emission tomography (PET) and single photon emission computed tomography (SPECT) could lead to the presymptomatic detection of AD and new anti-amyloid therapies.[3-5]

In the past few years, several groups have reported potential Aβ-imaging probes for the detection of Aβ plaques *in vivo*. Tracers such as [^{11}C]PIB,[6,7] [^{11}C]SB-13,[8,9] [^{18}F]BAY94-9172,[10] [^{11}C]BF-227,[11] [^{18}F]FDDNP[12-14] and [^{123}I]IMPY[15-18] have been tested clinically and demonstrated utility. [^{123}I]IMPY is the only tracer for SPECT, the

other 5 tracers are Aβ-imaging probes for PET. Since SPECT is more valuable than PET in terms of routine diagnostic use, the development of more useful Aβ-imaging agents for SPECT has been a critical issue.

Recently, we successfully designed and synthesized a new series of 3,5-diphenyl-1,2,4-oxadiazole (1,2,4-DPOD) derivatives as SPECT probes for the *in vivo* imaging of Aβ plaques in the brain.[19] The 1,2,4-DPOD derivatives are categorized into Aβ-imaging agents with the three-aromatic-ring linked system.[20-22] The derivatives displayed excellent affinity for Aβ aggregates in *in vitro* binding experiments. The degree to which the DPOD derivatives penetrated the brain was also very encouraging. However, nonspecific binding *in vivo* reflected by a slow washout from the normal mouse brain makes them unsuitable for the imaging of Aβ plaques. The less than ideal *in vivo* biodistribution results in normal mice indicate that there is a critical need to fine-tune the kinetics of brain uptake and washout. Additional structural changes, i.e. reducing the lipophilicity, are necessary to improve the *in vivo* properties of the DPOD derivatives.

In an attempt to further develop novel ligands for the imaging of Aβ plaques in AD, we designed a series of 2,5-diphenyl-1,3,4-oxadiazole (1,3,4-DPOD) derivatives, which are structural isomers of 1,2,4-DPOD and less lipophilic than 1,2,4-DPOD (Fig. 1). To our knowledge, this is the first time the use of 1,3,4-DPOD derivatives *in vivo* as probes to image Aβ plaques in the AD brain has been proposed. Described herein is the synthesis of a novel series of 1,3,4-DPOD derivatives and the characterization as Aβ imaging probes in comparison with 1,2,4-DPOD derivatives.

2. Results and Discussion

The synthesis of 1,3,4-DPOD derivatives is outlined in Schemes 1 and 2. We used the one-pot synthesis method of producing 2,5-diphenyl-1,3,4-oxadiazoles.[23] The 2,5-diphenyl-1,3,4-oxadiazoles (**3** and **4**) were prepared by 4-iodobenzhydrazide with 4-dimethylaminobenzaldehyde and 4-meyhoxybenzaldehyde in the presence of ceric ammonium nitrate (CAN). Compound **4** was converted to **6** by demethylation with BBr_3 in CH_2Cl_2 (49% yield). Direct alkylation of **6** with ethylene chlorohydrin, ethylene

glycol mono-2-chloroethyl ether, or 2-[2-(2-choloroethoxy)ethoxy]ethanol with potassium carbonate in DMF resulted in **7**, **8** and **9**. The tributyltin derivatives (**2** and **5**) were prepared from corresponding compounds (**1** and **4**) using a halogen to tributyltin exchange reaction catalyzed by Pd(0) for yields of 8.2% and 6.5%, respectively. The tributyltin derivatives were used as the starting materials for radioiodination in the preparation of [^{125}I]**3** and [^{125}I]**4**. Novel radioiodinated 1,3,4-DPOD derivatives were obtained by an iododestannylation reaction using hydrogen peroxide as the oxidant which produced the desired radioiodinated ligands (Scheme 3). It was anticipated that the no-carrier-added preparation would result in a final product bearing a theoretical specific activity similar to that of ^{125}I (2200 Ci/mmol). The radiochemical identity of the radioiodinated ligands was verified by co-injection with non-radioiodinated compounds from their HPLC profiles. [^{125}I]**3** and [^{125}I]**4** were each obtained in a radiochemical yield of >45% with a radiochemical purity of >95% after purification by HPLC.

The affinity of 1,3,4-DPOD derivatives (**3**, **4**, **6**, **7**, **8** and **9**) was evaluated based on inhibition of the binding of [^{125}I]IMPY to Aβ42 aggregates. As shown in Table 1, all

1,3,4-DPOD derivatives showed inhibitory activity toward Aβ aggregates. The affinity of 1,3,4-DPOD derivatives for Aβ aggregates varied from 20 to 349 nM. Compound **3** with the dimethylamino group and **4** with the methoxy group showed high binding affinity with a K_i of 20 and 46 nM, respectively, while no marked affinity was observed for **6**, **7**, **8** and **9**. Compound **3** displayed almost equal affinity for Aβ aggregates as the 1,2,4-DPOD derivative with the dimethylamino group (4-(3-(4-iodophenyl)-1,2,4-oxadiazole-5-yl)-*N,N*-dimethylamine; 1,2,4-DPOD-DM, K_i= 15 nM).[19]

To confirm the affinity of 1,3,4-DPOD derivatives for Aβ plaques in the brain, fluorescent staining of sections of mouse brain from an animal model of AD was carried out with compound **3** (Fig. 2). Many fluorescence spots were observed in the brain sections of Tg2576 transgenic mice (female, 28-month-old) (Fig. 2-A), while no spots were observed in the brain sections of wild-type mice (female, 28-month-old) (Fig. 2-B). The fluorescent labeling pattern was consistent with that observed with thioflavin S (Fig. 2-C). These results suggested that **3** shows specific binding to Aβ plaques in the mouse

brain. In the fluorescent staining of Tg2576 mouse brain sections, **4** also showed specific binding to Aβ plaques in the brain (data not shown).

Next, [^{125}I]**3** and [^{125}I]**4** were evaluated for their *in vivo* biodistribution in normal mice. A biodistribution study provides critical information on brain penetration. Generally, a freely diffusible compound with an optimal log P value of 2−3 will have an initial brain uptake of 2−3% dose/whole brain at 2 min after iv injection. [^{125}I]**3** and [^{125}I]**4** examined in this study displayed optimal lipophilicity as reflected by log P values of 2.43 and 2.58, respectively (Table 2). As expected, these ligands displayed good brain uptake ranging from 3.8 to 5.9% ID/g brain at 2-10 min postinjection, indicating a level sufficient for brain imaging probes (Table 3). In addition, they displayed good clearance from the normal brain with 1.8 and 0.36% ID/g at 60 min postinjection for [^{125}I]**3** and [^{125}I]**4**, respectively. These values were equal to a peak in brain uptake of 30 and 9.6%, respectively. Additionally, all of the other organs or tissues displayed a good initial uptake and a relatively fast washout with time. To directly compare the brain uptake and washout of [^{125}I]1,2,4-DPOD and

[^{125}I]1,3,4-DPOD, a combined plot is presented in Figure 3. It is apparent that [^{125}I]1,2,4-DPOD showed a lower initial uptake with a longer retention, while [^{125}I]1,3,4-DPOD displayed a higher initial uptake but with a faster washout from the brain. At 2 or 10 minutes after iv injection, the uptake of [^{125}I]1,3,4-DPOD reached a maximum after which the activity in the normal brain was washed out. It is important to note that the ideal Aβ imaging agent should have good brain penetration to deliver the intended dose into the brain, while maintaining a fast washout from normal tissues. Because the normal brain has no Aβ plaques to trap the agent, the washout from the brain should also be fast. Once the high affinity ligand is delivered into the regions containing the Aβ plaques, imaging agents such as [^{125}I]**3** and [^{125}I]**4** are expected to be trapped in this region longer due to its high binding affinity. The differences between the kinetics in normal and Aβ plaque-containing regions will result in a higher signal to noise ratio (target to non-target ratio) in the AD brain. Based on the data presented for [^{125}I]1,3,4-DPOD, it is predicted that the brain trapping of [^{125}I]1,3,4-DPOD in Aβ-containing regions will be much better than that of [^{125}I]1,2,4-DPOD. The log P

values of 1,3,4-DPOD derivatives (log P = 2.43 and 2.58 for **3** and **4**, respectively) were lower than those of 1,2,4-DPOD derivatives (log P = 3.22 and 3.37 for 1,2,4-DPOD-DM and 1,2,4-DPOD-OMe, respectively). Although many factors such as molecular size, ionic charge, and lipophilicity affect the uptake of a compound into the brain, the difference in lipophilicility may be one reason for the difference in brain uptake and washout between 1,3,4-DPOD and 1,2,4-DPOD. Further structural modifications, i.e. decreasing the lipophilicity by introducing the hydrophilic group, should improve the *in vivo* properties of 1,3,4-DPOD derivatives.

3. Conclusion

In conclusion, we successfully designed and synthesized a new series of 1,3,4-DPOD derivatives as probes for the *in vivo* imaging of Aβ plaques in the brain. In *in vitro* binding experiments, these 1,3,4-DPOD derivatives showed affinity for Aβ42 aggregates. The 1,3,4-DPOD derivatives clearly stained Aβ plaques in an animal model of AD, reflecting their affinity for Aβ aggregates *in vitro*. Compared to 1,2,4-DPOD, they displayed good penetration of and a fast washout from the brain in biodistribution

experiments using normal mice. Taken together, the present results suggested that the novel radioiodinated 1,3,4-DPOD derivatives may be useful probes for detecting Aβ plaques in the AD brain.

4. Experimental

4.1. General

All reagents were commercial products and used without further purification unless otherwise indicated. ^{1}H NMR spectra were obtained on a Varian Gemini 300 spectrometer with TMS as an internal standard. Coupling constants are reported in Hertz. Multiplicity is defined by s (singlet), d (doublet), t (triplet), and m (multiplet). ^{13}C NMR spectra were obtained on an AL400 JEOL spectrometer with TMS as an internal standard. Mass spectra were obtained on a JEOL IMS-DX.

4.1.1. 4-(5-(4-Bromophenyl)-1,3,4-oxadiazol-2-yl)-*N*,*N*-dimethylbenzenamine (1).

To a solution of 4-bromobenzhydrazine (215 mg, 1 mmol) and

4-dimethylaminobenzaldehyde (149 mg, 1 mmol) in dry CH_2Cl_2 (10 mL) was added CAN (548 mg, 1 mmol). The reaction mixture was stirred under reflux for 24 h. Water was added and following extraction with $CHCl_3$, the organic phase was dried over Na_2SO_4. The solvent was removed and the residue was purified by silica gel chromatography (hexane : ethyl acetate = 4:1) to give 12 mg of **1** (3.5%). ^{1}H NMR (300 MHz, $CDCl_3$) δ 3.08 (s, 6H), 6.76 (d, *J* = 9.0 Hz, 2H), 7.66 (d, *J* = 8.4 Hz, 2H), 7.98 (dd, *J* = 5.4, 4.5 Hz, 4H). MS m/z 362 (M^+).

4.1.2.

4-(5-(4-Tributylstannyl)phenyl)-1,3,4-oxadiazol-2-yl)-*N,N*-dimethylbenzenamine (2).

A mixture of **1** (19 mg, 0.06 mmol), bis(tributyltin) (0.04 mL) and $(Ph_3P)_4Pd$ (3 mg, 0.002 mmol) in a mixed solvent (6 mL, 1:1 dioxane/Et_3N) was stirred under reflux for 4.5 h. The solvent was removed, and the residue was purified by silica gel chromatography (hexane : ethyl acetate = 3 : 1) to give 2.5 mg of **2** (8.2%). ^{1}H NMR

(300 MHz, $CDCl_3$) δ 0.87-1.6 (m, 27H), 3.07 (s, 6H), 6.77 (d, *J* = 9.0 Hz, 2H), 7.61 (d, *J* = 8.4 Hz, 2H), 8.01 (dd, *J* = 9.0, 8.1 Hz, 4H).

4.1.3. 4-(5-(Iodophenyl)-1,3,4-oxadiazol-2-yl)-*N*,*N*-dimethylbenzenamine (3).

The same reaction as described above to prepare **1** was used, and 14 mg of **3** was obtained in a 1.8% yield from 4-iodobenzohydrazide and 4-dimethylaminobenzaldehyde. ^{1}H NMR (300 MHz, $CDCl_3$) δ 3.07 (s, 6H), 6.76 (d, *J* = 3.0 Hz, 2H), 7.85 (d, *J* = 12.0 Hz, 4H), 7.97 (d, *J* = 3.0 Hz, 2H). ^{13}C NMR (400 MHz, $CDCl_3$) δ 165.5, 162.9, 152.5, 138.2, 128.4, 128.0, 123.9, 111.6, 110.7, 97.8, 40.1. HRMS m/z $C_{16}H_{14}N_3OI$ found 391.0191/ calcd 391.0182 (M^+).

4.1.4. 2-(4-Iodophenyl)-5-(4-methoxyphenyl)-1,3,4-oxadiazole (4).

The same reaction as described above to prepare **1** was used, and 40 mg of **4** was obtained in a 8.8% yield from 4-iodobenzohydrazide and 4-methoxybenzaldehyde. ^{1}H NMR (300 MHz, $CDCl_3$) δ 3.89 (s, 3H), 7.03 (d, *J* = 2.9 Hz, 2H), 7.86 (q, *J* = 7.8 Hz,

4H), 8.03 (d, *J* = 3.0 Hz, 2H). ^{13}C NMR (400 MHz, $CDCl_3$) δ 164.7, 163.6, 162.5, 138.3, 128.8, 128.1, 123.6, 116.2, 114.6, 98.2, 55.5. HRMS m/z $C_{15}H_{11}N_2O_2I$ found 377.9877/ calcd 377.9865 (M^+).

4.1.5. 2-(4-(Tributylstannyl)phenyl)-5-(4-meyhoxyphenyl)-1,3,4-oxadiazole (5).

The same reaction as described above to prepare **2** was used, and 6 mg of **5** was obtained in a 6.5% yield from **4**. ^{1}H NMR (300 MHz, $CDCl_3$) δ 0.87-1.58 (m, 27H), 3.91 (s, 3H), 7.04 (d, *J* = 3.1 Hz, 2H), 7.63 (d, *J* = 2.6 Hz, 2H), 8.06 (q, *J* = 6.6 Hz, 4H).

4.1.6. 4-(5-(4-Iodophenyl)-1,3,4-oxadiazol-2-yl)phenol (6).

BBr_3 (0.6 mL, 1 M solution in CH_2Cl_2) was added to a solution of **4** (36 mg, 0.1 mmol) in CH_2Cl_2 (16 mL) dropwise in an ice bath. The mixture was allowed to warm to room temperature and stirred for 5 days. Water (50 mL) was added while the reaction mixture was cooled in an ice bath. The mixture was extracted with $CHCl_3$ (30 mL) and the water layer was extracted with ethyl acetate. The organic phase was dried over Na_2SO_4 and

filtered. The solvent was removed, and the residue was purified by silica gel chromatography (hexane : ethyl acetate = 2 : 1) to give 17 mg of **6** (49.0%). ^{1}H NMR (300 MHz, $CDCl_3$) δ 6.98-7.06 (m, 2H), 7.86-7.91 (m, 4H), 8.02-8.09 (m, 2H). HRMS m/z $C_{14}H_9N_2O_2I$ found 363.9712/ calcd 363.9709 (M^+).

4.1.7. 2-(4-(5-(4-Iodophenyl)-1,3,4-oxadiazol-2-yl)phenoxy)ethanol (7).

A mixture of **6** (22 mg, 0.06 mmol), potassium carbonate (24.5 mg, 0.18 mmol) and ethylene chlorohydrin (4 μL, 0.06 mmol) in anhydrous DMF (3 mL) was stirred under reflux for 6.5 h. After cooling to room temperature, water was added, and the reaction mixture was extracted with $CHCl_3$. The organic layer was separated, dried over Na_2SO_4 and evaporated. The resulting residue was purified by silica gel chromatography (hexane : ethyl acetate = 2 : 3) to give 11 mg of **7** (44.6%). ^{1}H NMR (300 MHz, $CDCl_3$) δ 4.03 (q, *J* = 5.0 Hz, 2H), 4.18 (d, *J* = 3.0 Hz, 2H) 7.06 (d, *J* = 3.0 Hz, 2H), 7.87 (q, *J* = 8.0 Hz, 4H), 8.07 (d, *J* = 3.0 Hz, 2H). HRMS m/z $C_{16}H_{13}N_2O_3I$ found 407.9983/ calcd 407.9971 (M^+).

4.1.8. 2-(2-(4-(5-(4-Iodophenyl)-1,3,4-oxadiazol-2-yl)phenoxy)ethoxy)ethanol (8).

The same reaction as described above to prepare **7** was used, and 9 mg of **8** was obtained in a 25.9% yield from **6** and ethylene glycol mono-2-chloroethyl ether. ^{1}H NMR (300 MHz, $CDCl_3$) δ 3.70 (t, *J* = 3.1 Hz, 2H), 3.79 (q, *J* = 4.8Hz, 2H), 3.92 (t, *J* = 3.2Hz, 2H), 4.23 (t, *J* = 3.1Hz, 2H), 7.06 (d, *J* = 3.1 Hz, 2H), 7.87 (q, *J* = 7.6 Hz, 4H), 8.70 (d, *J* = 3.1 Hz, 2H). HRMS m/z $C_{18}H_{17}N_2O_4I$ found 452.0244/ calcd 452.0233 (M^+).

4.1.9.

2-(2-(2-(4-(5-(4-Iodophenyl)-1,3,4-oxadiazol-2-yl)phenoxy)ethoxy)ethoxy)ethanol (9).

The same reaction as described above to prepare **7** was used, and 7.8 mg of **9** was obtained in a 44.7% yield from **6** and 2-[2-(chloroethoxy)ethoxy]ethanol. ^{1}H NMR (300 MHz, $CDCl_3$) δ 3.61-3.77 (m, 8H), 3.91 (t, *J* = 3.1Hz), 4.23 (t, *J* = 3.2Hz, 2H), 7.06 (d, *J* = 3.0 Hz, 2H), 7.87 (q, *J* = 7.8 Hz, 4H), 8.06 (d, *J* = 2.3 Hz, 2H). HRMS m/z

$C_{20}H_{21}N_2O_5I$ found 496.0525/ calcd 496.0495 (M^+).

4.2. Iododestannylation reaction

The radioiodinated forms of compounds **3** and **4** were prepared from the corresponding tributyltin derivatives by iododestannylation. Briefly, to initiate the reaction, 50 μL of H_2O_2 (3%) was added to a mixture of a tributyltin derivative (50 μg/50 μL EtOH), [^{125}I]NaI (0.1–0.2 mCi, specific activity 2200 Ci/mmol), and 50 μL of 1 N HCl in a sealed vial. The reaction was allowed to proceed at room temperature for 3 min and terminated by addition of $NaHSO_3$. After neutralization with sodium biocarbonate and extraction with ethyl acetate, the extract was dried by passing through an anhydrous Na_2SO_4 column and then blown dry with a stream of nitrogen gas. The radioiodinated ligand was purified by HPLC on a Cosmosil C_{18} column with an isocratic solvent of H_2O/acetonitrile (4:6) at a flow rate of 1.0 mL /min.

4.3. Binding assays using the aggregated Aβ peptide in solution.

A solid form of Aβ42 was purchased from Peptide Institute (Osaka, Japan). Aggregation was carried out by gently dissolving the peptide (0.25 mg/mL) in a buffer solution (pH 7.4) containing 10 mM sodium phosphate and 1 mM EDTA. The solution was incubated at 37 ℃ for 42 h with gentle and constant shaking. Binding assays were carried out as described previously.[24] [^{125}I]IMPY (6-iodo-2-(4'-dimethylamino)phenyl-imidazo[1,2]pyridine) with 2200 Ci/mmol specific activity and greater than 95% radiochemical purity was prepared using the standard iododestannylation reaction as described previously.[15] Binding assays were carried out in 12 × 75 mm borosilicate glass tubes. A mixture containing 50 μL of test compound (0.2 pM - 400 μM in 10% EtOH), 50 μL of [^{125}I]IMPY (0.02 nM diluted in 10%EtOH), 50 μL of Aβ42 aggregates, and 850 μL of 10% ethanol was incubated at room temperature for 3 h. The mixture was then filtered through Whatman GF/B filters using a Brandel M-24 cell harvester, and the filters containing the bound ^{125}I ligand were placed in a gamma counter (Aloka, ARC-380). Values for the half-maximal

inhibitory concentration (IC_{50}) were determined from displacement curves of three independent experiments using GraphPad Prism 4.0, and those for the inhibition constant (K_i) were calculated using the Cheng-Prusoff equation.[25]

4.4. Neuropathological staining of model mouse brain sections

The experiments with animals were conducted in accordance with our institutional guidelines and were approved by Nagasaki University Animal Care Committee. The Tg2576 transgenic mice (female, 28-month-old) and wild-type mice (female, 28-month-old) were used as the Alzheimer's model and control mice, respectively. After the mice were sacrificed by decapitation, the brains were immediately removed and frozen in powdered dry ice. The frozen blocks were sliced into serial sections, 10 μm thick. Each slide was incubated with a 50% EtOH solution (100 μM) of compounds **3** and **4** for 30 min. The sections were washed in 50% EtOH for 1 min two times, and examined using a microscope (Nikon Eclipse 80i) equipped with a UV-1A filter set (excitation, 365-375 nm; diachronic mirror, 400 nm; longpass filter, 400 nm). Thereafter,

the serial sections were also stained with thioflavin S, a pathological dye commonly used for staining Aβ plaques in the brain, and examined using a microscope (Nikon Eclipse 80i) equipped with a B-2A filter set (excitation, 450-480 nm; diachronic mirror, 505 nm; longpass filter, 520 nm).

4.5. Determination of Partition coefficient determination

Partition coefficients were measured by mixing [^{125}I]**3** and [^{125}I]**4** with 1.5 mL each of 1-octanol and buffer (0.1 M phosphate, pH 7.4) in a test tube. The test tube was vortexed for 20 sec three times. Two weighed samples (1mL each) from the 1-octanol and buffer layers were measured for radioactivity with a gamma counter. The partition coefficient was determined by calculating the ratio of cpm/1mL of 1-octanol to that of the buffer.

4.6. *In vivo* biodistribution in normal mice.

A saline solution (100 μL) of radiolabeled agents (0.2 – 0.4 μCi) containing ethanol

(10 μL) was injected intravenously directly into the tail of ddY mice (5-week-old, 22-25 g). The mice were sacrificed at various time points post-injection. The organs of interest were removed and weighed, and radioactivity was measured with an automatic gamma counter (Aloka, ARC-380).

Acknowledgements

This study was supported by the Program for Promotion of Fundamental Studies in Health Sciences of the National Institute of Biomedical Innovation (NIBIO) and a Health Labour Sciences Research Grant.

References

1. Klunk, W. E. *Nurobiol. Aging* **1998**, *19*, 145.

2. Hardy, J.; Selkoe, D. J. *Science* **2002**, *297*, 353.

3. Mathis, C. A.; Lopresti, B. J.; Klunk, W. E. *Nucl. Med. Biol.* **2007**, *34*, 809.

4. Mathis, C. A.; Wang,Y.; Klunk, W. E. *Curr. Pharm. Des.* **2004**, *10*, 1469.

5. Nordberg, A. *Lancet Neurol.* **2004**, *3*, 519

6. Mathis, C. A.; Wang, Y.; Holt, D. P.; Huang, G. F.; Debnath, M. L.; Klunk, W. E. *J. Med. Chem.* **2003**, *46*, 2740.

7. Klunk, W. E.; Engler, H.; Nordberg, A.; Wang, Y.; Blomqvist, G.; Holt, D. P.; Bergstrom, M.; Savitcheva, I.; Huang, G. F.; Estrada, S.; Ausen, B.; Debnath, M. L.; Barletta, J.; Price, J. C.; Sandell, J.; Lopresti, B. J.; Wall, A.; Koivisto, P.; Antoni, G.; Mathis, C. A.; Langstrom, B. *Ann. Neurol.* **2004**, *55*, 306.

8. Ono, M.; Wilson, A.; Norbrega, J.; Westaway, D.; Verhoeff, P.; Zhuang, Z. P.; Kung, M. P.; Kung, H. F. *Nucl. Med. Biol.* **2003**, *30*, 565

9. Verhoeff, N. P.; Wilson, A. A.; Takeshita, S.; Trop, L.; Hussey, D.; Singh, K. Kung, H.

F.; Kung, M. P.; Houle, S. *Am. J. Geriatr. Psychiatry* **2004**, *12*, 584.

10. Rowe, C. C.; Ackerman, U.; Browne, W.; Mulligan, R.; Pike, K. L.; O'Keefe, G.; Tochon-Danguy, H.; Chan, G.; Berlangieri, S. U.; Jones, G.; Dickinson-Rowe, K. L.; Kung, H. P.; Zhang, W.; Kung, M. P.; Skovronsky, D.; Dyrks, T.; Holl, G.; Krause, S.; Friebe, M.; Lehman, L.; Lindemann, S.; Dinkelborg, L. M.; Masters, C. L.; Villemagne, V.L. *Lancet Neurol.* **2008**, *7*, 129.

11. Kudo, Y.; Okamura, N.; Furumoto, S.; Tashiro, M.; Furukawa, K.; Maruyama, M.; Itoh, M.; Iwata, R.; Yanai, K.; Arai, H. *J. Nucl. Med.* **2007**, *48*, 553.

12. Agdeppa, E. D.; Kepe, V.; Liu, J.; Flores-Torres, S.; Satyamurthy, N.; Petric, A.; Cole, G. M.; Small, C. W.; Huang, S. C.; Barrio, J. R. *J. Nurosci.* **2001**, *21*, RC189.

13. Shoghi-Jadid, K.; Small, G. W.; Agdeppa, E. D.; Kepe, V.; Ercoli, L. M.; Siddarth, P.; Read, S.; Satyamurthy, N.; Petric, A.; Huang, S. C.; Barrio, J. R. *Am. J. Geriatr. Psychiatry* **2002**, *10*, 24.

14. Small, G. W.; Kepe, V.; Ercoli, L. M.; Siddarth, P.; Bookheimer, S. Y.; Miller, K. J.; Lavretsky, H.; Burggren, A. C.; Cole, G. M.; Vinters, H. V.; Thompson, P. M.; Huang,

S. C.; Satyamurthy, N.; Phelps, M. E.; Barrio, J. R. *N. Engl. J. Med.* **2006**, *355*, 2652.

15. Kung, M. P.; Hou, C.; Zhuang, Z. P.; Zhang, B.; Skovronsky, D.; Trojanowski, J. Q.; Lee, V. M.; Kung, H. F. *Brain Res*. **2002**, *956*, 202.

16. Zhuang, Z. P.; Kung, M. P.; Wilson, A.; Lee, C. W.; Plossl, K.; Hou, C.; Holtzman, D. M.; Kung, H. F. *J. Med. Chem*. **2003**, *46*, 237.

17. Newberg, A. B.; Wintering, N. A.; Plossl, K.; Hochold, J.; Stabin, M. G.; Watson, M.; Skovronsky, D.; Clark, C. M.; Kung, M. P.; Kung, H. F. *J. Nucl. Med.* **2006**, *47*, 748.

18. Newberg, A. B.; Wintering, N. A.; Clark, C. M.; Plossl, K.; Skovronsky, D.; Seibyl, J. P.; Kung, M. P.; Kung, H. F. *J. Nucl. Med.* **2006**, *47*, 78P.

19. Ono, M.; Haratake, M.; Saji, H.; Nakayama, M. *Bioorg. Med. Chem.* **2008**, *16*, 6867.

20. Neaterov, E. E.; Skoch, J.; Hyman, B. T.; Klunk, W. E.; Bacskai, B. J.; Swager, T. M. *Angew. Chem. Int*. **2005**, *44*, 5452.

21. Chabdra, R.; Kung, M. P.; Kung, H.F. *Bioorg. Med. Chem. Lett*. **2006**, *16*, 1350.

22. Qu, W.; Kung, M. P.; Hou. C.; Oya, S.; Kung, H. F. *J. Med. Chem*. **2007**, *50*, 3380.

23. Dabiti, M.; Salehi, P.; Baghbanzadeh, M.; Bahramnejad, M. *Tetrahedron Lett.* **2006**, *47*, 6983.

24. Kung, M. P.; Hou, C.; Zhuang, Z. P.; Skovronsky, D.; Kung, H. F. *Brain Res.* **2004**, *1025*, 98.

25. Cheng, Y.; Prusoff, W. H.; *Biochem. Pharmacol.* **1973**, *22*, 3099.

Table 1. Inhibition constants (K_i) for binding of 1,3,4-DPOD derivatives determined using [^{125}I]IMPY as the ligand in Aβ42 aggregates.

Compound	K_i (nM)[a]
3	20.1 ± 2.5
4	46.1 ± 12.6
6	229.6 ± 47.3
7	282.2 ± 61.4
8	348.6 ± 51.7
9	257.7 ± 34.8

[a]Values are the mean ± standard error for the mean for 4-6 independent experiments.

Table 2. Partition coefficients for 1,2,4-DPOD and 1,3,4-DPOD derivatives.

Compound	log P^a
3	2.43 ± 0.07
4	2.58 ± 0.06
1,2,4-DPOD-DM	3.22 ± 0.01
1,2,4-DPOD-OMe	3.37 ± 0.04

[a]Octanol/buffer (0.1 M phosphate-buffered saline, pH 7.4) partition coefficients. Each value represents the mean (SD) for 2-3 experiments.

Table 3. Biodistribution of radioactivity after injection of [^{125}I]1,3,4-DPOD derivatives in normal mice[a].

	Time after injection (min)			
Tissue	2	10	30	60
		[^{125}I]**3**		
Blood	3.28 (0.46)	3.51 (0.29)	2.53 (0.28)	2.21 (0.41)
Liver	15.87 (3.49)	19.12 (2.43)	12.64 (2.44)	10.01 (1.64)
Kidney	9.14 (1.60)	7.80 (0.64)	5.71 (1.35)	3.81 (0.64)
Intestine	2.28 (0.55)	11.34 (1.61)	12.58 (2.35)	16.22 (2.51)
Spleen	3.56 (0.96)	4.10 (0.40)	2.63 (0.54)	2.05 (0.41)
Pancreas	5.32 (0.98)	4.39 (2.17)	2.50 (0.56)	2.14 (0.90)
Heart	3.99 (3.10)	3.55 (1.86)	2.03 (0.30)	1.54 (0.31)
Stomach[b]	1.40 (0.10)	4.73 (1.86)	4.79 (1.12)	5.50 (0.51)
Brain	2.98 (0.53)	5.93 (0.76)	3.16 (0.69)	1.78 (0.41)
		[^{125}I]**4**		
Blood	1.84 (0.30)	1.60 (0.30)	1.26 (0.26)	0.80 (0.20)
Liver	9.60 (1.73)	12.60 (1.14)	8.07 (1.66)	4.65 (1.34)
Kidney	7.14 (1.46)	4.85 (0.48)	4.36 (1.12)	2.48 (0.37)
Intestine	2.07 (0.36)	4.49 (0.60)	10.06 (1.81)	19.85 (4.71)
Spleen	2.44 (0.28)	1.51 (0.26)	0.80 (0.10)	0.60 (0.26)
Pancreas	4.74 (0.63)	1.98 (0.37)	0.96 (0.03)	0.57 (0.14)
Heart	4.80 (1.33)	1.73 (0.27)	0.92 (0.25)	0.43 (0.11)
Stomach[b]	0.71 (0.13)	1.41 (0.91)	3.12 (0.90)	2.90 (1.57)
Brain	3.75 (0.78)	2.74 (0.37)	1.04 (0.14)	0.36 (0.13)

[a]Expressed as % injection dose per gram. Each value represents the mean (SD) for 4-6 animals.

[b]Expressed as % injected dose per organ.

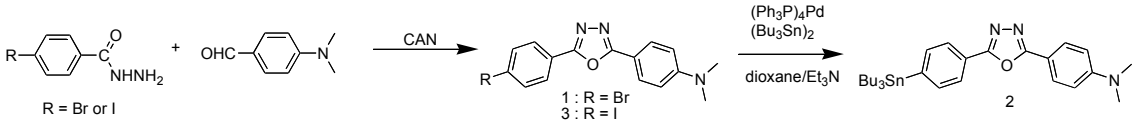
R
O
C
NHNH2
R = Br or I
+
OHC
N
CAN
N–N
O
R
N
1 : R = Br
3 : R = I
(Ph3P)4Pd
(Bu3Sn)2
dioxane/Et3N
N–N
O
Bu3Sn
N
2

Scheme 1

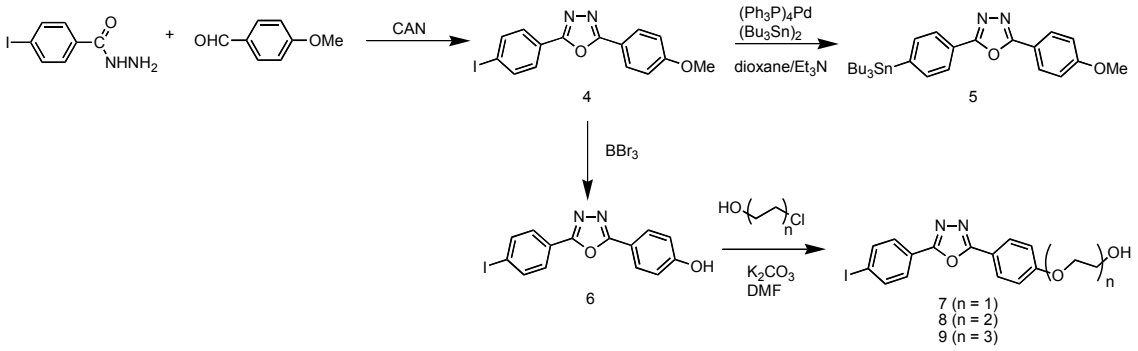
I
O
C
NHNH2
+
OHC
OMe
CAN
N–N
O
I
OMe
4
(Ph3P)4Pd
(Bu3Sn)2
dioxane/Et3N
Bu3Sn
OMe
5
BBr3
I
OH
6
HO
n
Cl
K2CO3
DMF
OH
7 (n = 1)
8 (n = 2)
9 (n = 3)

Scheme 2

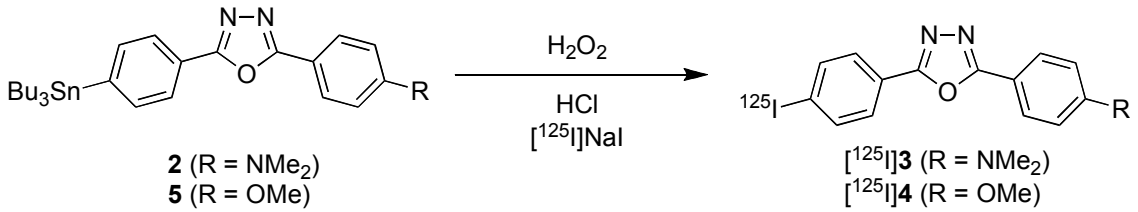

2 (R = NMe_2)
5 (R = OMe)

[^{125}I]**3** (R = NMe_2)
[^{125}I]**4** (R = OMe)

Scheme 3

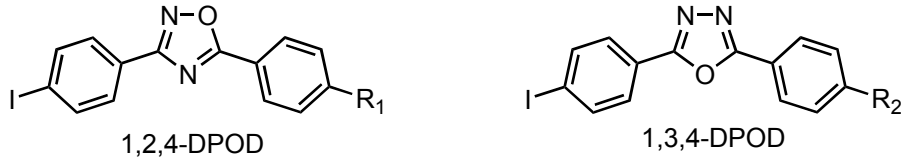

Figure 1. Chemical structure of 1,2,4-DPOD reported previously and 1,3,4-DPOD reported in this paper. R_1= NH_2, $NHCH_3$, $N(CH_3)_2$, OCH_3, OH; R_2 = $N(CH_3)_2$, OCH_3, OH, OCH_2CH_2OH, $(OCH_2CH_2)_2OH$, $(OCH_2CH_2)_3OH$.

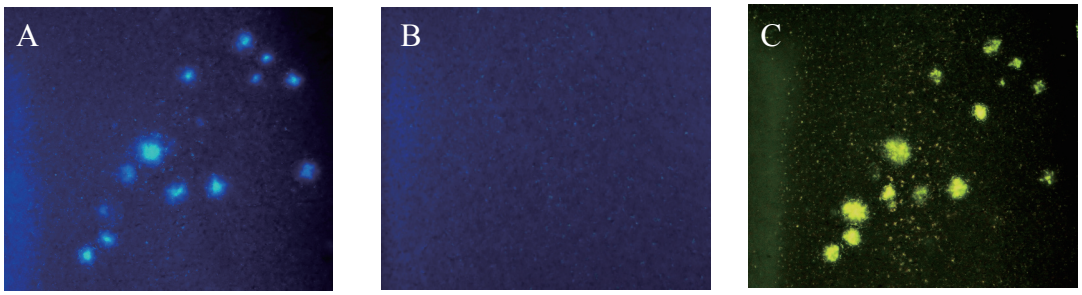

Figure 2. Neuropathological staining of compound **3** on 10-μm AD model mouse sections (A) and wild-type mouse sections (B). Labeled plaques were confirmed by staining of the adjacent sections with thioflavin S (C).

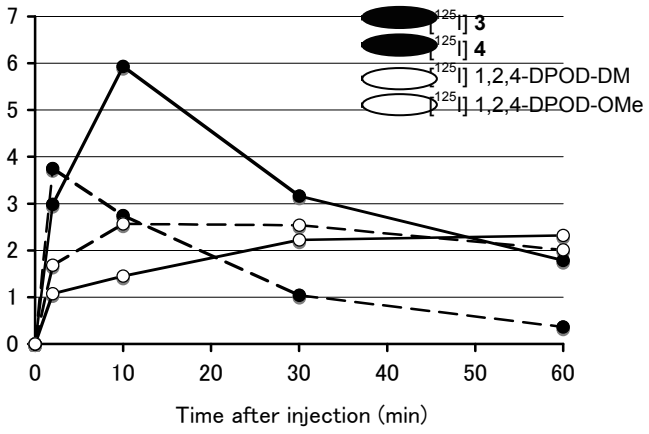

Figure 3. Comparison of brain uptake of [^{125}I]**3**, [^{125}I]**4**, [^{125}I]1,2,4-DPOD-DM and [^{125}I]1,2,4-DPOD-OMe in normal mice. The kinetics of the uptake of [^{125}I]**3** and [^{125}I]**4** may provide a better pattern for the localization of Aβ plaques in the brain.